



University of Kentucky
UKnowledge

Forestry and Natural Resources Faculty
Publications

Forestry and Natural Resources

12-12-2018

Dynamics of Postfire Aboveground Carbon in a Chronosequence of Chinese Boreal Larch Forests

Yuan Z. Yang

Guangxi Teachers Education University, China

Wen H. Cai

Guangxi Teachers Education University, China

Jian Yang

University of Kentucky, jian.yang@uky.edu

Megan White


University of Kentucky

John M. Lhotka

University of Kentucky, jmlhot2@uky.edu

Right click to open a feedback form in a new tab to let us know how this document benefits you.

Follow this and additional works at: https://uknowledge.uky.edu/forestry_facpub

 Part of the [Forest Sciences Commons](#), [Natural Resource Economics Commons](#), [Natural Resources and Conservation Commons](#), and the [Natural Resources Management and Policy Commons](#)

Repository Citation

Yang, Yuan Z.; Cai, Wen H.; Yang, Jian; White, Megan; and Lhotka, John M., "Dynamics of Postfire Aboveground Carbon in a Chronosequence of Chinese Boreal Larch Forests" (2018). *Forestry and Natural Resources Faculty Publications*. 28.
https://uknowledge.uky.edu/forestry_facpub/28

This Article is brought to you for free and open access by the Forestry and Natural Resources at UKnowledge. It has been accepted for inclusion in Forestry and Natural Resources Faculty Publications by an authorized administrator of UKnowledge. For more information, please contact UKnowledge@lsv.uky.edu.

Dynamics of Postfire Aboveground Carbon in a Chronosequence of Chinese Boreal Larch Forests

Notes/Citation Information

Published in *Journal of Geophysical Research: Biogeosciences*, v. 123, issue 12, p. 3490-3506.

©2018. American Geophysical Union. All Rights Reserved.

The copyright holder has granted the permission for posting the article here.

Digital Object Identifier (DOI)

<https://doi.org/10.1029/2018JG004702>

RESEARCH ARTICLE

10.1029/2018JG004702

Key Points:

- Postfire dynamics of aboveground carbon storage were depicted over a 200-year chronosequence in boreal larch forests
- Aboveground carbon transformed from a source to a sink after 30 years, and it took over 120 years to recover 80% of old-growth stands
- There was a positive relationship between aboveground carbon and stand density over the entire range of stand age classes

Supporting Information:

- Supporting Information S1
- Data Set S1

Correspondence to:

J. Yang,
jian.yang@uky.edu

Citation:

Yang, Y. Z., Cai, W. H., Yang, J., White, M., & Lhotka, J. M. (2018). Dynamics of postfire aboveground carbon in a chronosequence of Chinese boreal larch forests. *Journal of Geophysical Research: Biogeosciences*, 123, 3490–3506. <https://doi.org/10.1029/2018JG004702>

Received 28 JUL 2018

Accepted 2 NOV 2018

Accepted article online 20 NOV 2018

Published online 12 DEC 2018

Author Contributions:

Conceptualization: Jian Yang

Data curation: Yuan Z. Yang, Wen H. Cai

Formal analysis: Yuan Z. Yang

Funding acquisition: Jian Yang

Investigation: Yuan Z. Yang, Wen H. Cai

Methodology: Yuan Z. Yang, Wen H. Cai, Jian Yang

Resources: Jian Yang

Writing - original draft: Yuan Z. Yang

Writing - review & editing: Wen H. Cai, Jian Yang, Megan White, John M. Lhotka

Dynamics of Postfire Aboveground Carbon in a Chronosequence of Chinese Boreal Larch Forests

Yuan Z. Yang^{1,2,3} , Wen H. Cai^{1,2}, Jian Yang⁴ , Megan White⁴, and John M. Lhotka⁴

¹Key Laboratory of Environment Change and Resources Use in Beibu Gulf (Guangxi Teachers Education University), Ministry of Education, Nanning, P. R. China, ²Guangxi Key Laboratory of Earth Surface Processes and Intelligent Simulation (Guangxi Teachers Education University), Nanning, P. R. China, ³Institute of Applied Ecology, Chinese Academy of Sciences, Shenyang, China, ⁴Department of Forestry and Natural Resources, TP Cooper Building, University of Kentucky, Lexington, KY, USA

Abstract Boreal forests store a large proportion of the global terrestrial carbon (C), while wildfire plays a crucial role in determining their C storage and dynamics. The aboveground C (AC) pool is an important component of forest C stocks. To quantify the turning point (transforming from C source to C sink) and recovery time of postfire AC, and assess how stand density affects the AC, 175 plots from eight stand age classes were surveyed as a chronosequence in the Great Xing'an Mountains of Northeast China. Linear and nonlinear regression analyses were conducted to describe postfire AC recovery patterns. The results showed that (1) postfire AC exhibited a skewed U-shaped pattern with the turning point at approximately year 30, when the change rate of AC shifted from negative to positive, (2) it took more than 120 years for this forest ecosystem to recover 80% of AC in unburned old-growth (200 years) stands, and (3) there was an overall positive relationship between AC and stand density over the entire range of stand age classes; and such relationship was stronger during the early- and late-successional stages, but weaker ($p > 0.05$) during the midsuccessional stage. Although boreal larch forests have been C sinks under historical fire free intervals, predicted increases in fire frequency could potentially shift it to a C source. Understanding postfire AC dynamics in boreal larch forests is central to predicting C cycling response to wildfire and provides a framework for assessing ecosystem resilience to disturbance in this region.

Plain Language Summary Boreal forests store more than 32% of total global forest carbon (C), but this C pool is very susceptible to wildfires which are one of the most pervasive disturbances in the boreal biome. Identifying the dynamic trajectory and recovery pattern of postfire aboveground C (AC) storage is crucial for understanding the global ecological significance of wildfire disturbance. A total of 175 plots from eight stand age classes were surveyed in the Great Xing'an Mountains of Northeast China to quantify ecological resilience, and further examine the relationship between various components of AC and stand density throughout successional stages. Our data analysis showed that the AC pool could be a C source to the atmosphere for several decades following fire disturbances; and it would take more than a century for the AC to recover 80% of that in old-growth boreal larch forests in Northeastern China. Increases in fire frequency due to climate change and human activities will increase C emission, which may significantly influence the regional C budget. Stand density was considered as a positive factor on AC accumulation following wildfire, but this effect may be counteracted by variation in tree size due to site productivity in other successional stages.

1. Introduction

Boreal forests compose about 15% of terrestrial ecosystems (Gower et al., 2001) and store more than 32% of total global forest carbon (C; Pan et al., 2011). This forest biome has been characterized as a C sink with slow decomposition rate of litter (Harden et al., 2000; Luysaert et al., 2007, 2008) and plays a crucial role in mitigating climate change (Luo et al., 2015; Pan et al., 2011). Wildfire is one of the most pervasive natural disturbances in boreal forests (Kelly et al., 2013; Randerson et al., 2006; X. L. Wang et al., 2015), strongly influencing landscape variations of forest age and structure (Johnstone et al., 2010) as well as ecosystem functions such as C storage and sequestration (Harden et al., 2000; Kashian et al., 2013; Seedre et al., 2014). Climate driven models predict an overall increase of wildfire frequency in boreal forests before the end of the 21st

century (Girardin et al., 2009; Goetz et al., 2007; Z. H. Liu et al., 2012; Stephens et al., 2014), which will intensify fire-induced C losses. If the postfire C recovery cannot make up for such losses, it could potentially cause the system to transition from a C sink to a C source (Hayes et al., 2011; Stinson et al., 2011). Understanding the recovery patterns and driving mechanisms of postfire C dynamics is therefore an important step in predicting the response of boreal ecosystem functions and services to changes in climate, fire disturbance regimes, and surface energy budget (Amiro et al., 2006; Fang et al., 2015).

The aboveground C (AC) pool is an important variable for understanding contributions of forests to the global C budget (Berner et al., 2012; Houghton, 2005; Mack et al., 2008). Postfire AC is determined by the accumulation of live AC (LAC) and dead AC (DAC; Hurteau & Brooks, 2011; Janisch & Harmon, 2002; Taylor et al., 2007). Wildfires not only release C during burning, but also redistribute C from the LAC to DAC pools (e.g., pyrogenic C) which could persist for many decades due to slow decomposition rates in boreal systems (Bird et al., 2015; Bond-Lamberty et al., 2002; Santin et al., 2015). Postfire AC initially decreases due to C emission from decomposition of dead biomass, and then increases with stand age as trees reestablish (Rothstein et al., 2004; Wirth et al., 2002). During the early postfire stage, C accumulation in regenerated vegetation is often less than C lost through dead biomass decomposition (Amiro et al., 2010; Mkhabela et al., 2009); hence, the AC pool is often considered a C source to atmosphere at this stage (Chapin et al., 2006; S. G. Liu et al., 2011). As the forest stand redevelops, the LAC pool continues to increase and could offset C emission from decomposition of the DAC pool to a point that the AC pool is transitioning to a C sink (Kashian et al., 2013; Mkhabela et al., 2009). Although this overall U-shaped pattern of the postfire AC trajectory has been ascertained by many empirical studies, the curve's turning point, at which the postfire AC pool switches from a C source to a C sink, remains undefined in many ecosystems. In light of this pattern's important implications for C sequestration (Matamala et al., 2008), it is imperative to expand our research from quantifying the overall pattern of postfire AC trajectory to examining its specific attributes.

The postfire AC pool is not only transient, but also resilient from a broad temporal perspective (Gao et al., 2018; Mack et al., 2011; Wirth et al., 2002). Resilience is the capacity for a system to reorganize and recover to its previous state (Johnstone et al., 2016; Seidl et al., 2016). Estimating the time needed for a postfire ecosystem to recover to a previous state (i.e., recovery time) is essential, especially in the context of changing disturbance regimes (Harwell et al., 1977; Ortiz & Wolff, 2002). If the fire free interval becomes shorter than recovery time, the AC pool would not recover to its previous C storage capacity (Harvey et al., 2016a; Johnstone et al., 2016), hence altering its ecological role in global C cycling. Additionally, a long recovery time could increase the exposure risk of ecosystems to natural or anthropogenic hazards, such as repeated wildfires, nonnative species invasion, and land clearing (Harvey et al., 2016a; Seedre et al., 2014; Stevens & Latimer, 2015). With higher fire frequency, the nutrients that are lost will limit regrowth capacity, lowering the maximum potential for C storage in the region. Postfire AC resilience varies in different forest ecosystems, and its quantification is challenging, partially due to limited time span or coarse temporal resolution of the fire chronosequence data reported in previous empirical studies (Berner et al., 2012; Kaye et al., 2010; Mack et al., 2008; Vijayakumar et al., 2016).

In addition to variations in turning point and recovery time, the postfire AC trajectory could also fluctuate in response to stand density (Alexander, Mack, Goetz, Loranty, et al., 2012; Kashian et al., 2006). Spatial heterogeneities in fire severity and site condition can give rise to variations in postfire tree recruitment density through modifying seed availability and seed bed quality (Cai et al., 2013; Donato et al., 2009; Johnstone et al., 2010; Turner et al., 2004, 2016). This early postfire spatial heterogeneity in tree recruitment density may last for a long time during the fire free interval (Johnstone et al., 2004; Kashian et al., 2005; Shenoy et al., 2010). Studies have found dense stands accumulate more C in live trees AC (LTAC) at a higher rate than sparse stands during early successional stages in those ecosystems where high-severity crown fires dominate (Kashian et al., 2006; Turner et al., 2004). However, such a positive relationship for LTAC may not readily be extended to LAC or total AC, since LAC includes both trees and shrubs, total AC includes LAC and DAC. Furthermore, it is uncertain whether such relationships would be consistent throughout various successional stages and different boreal ecosystems (Alexander, Mack, Goetz, Loranty, et al., 2012; Osawa et al., 2010).

Most studies about postfire AC dynamics in subalpine and boreal forests have been conducted in North America (Alexander & Mack, 2015; Kashian et al., 2013; Law et al., 2003; Mack et al., 2008), while ecosystems in Eurasia have received less attention (Alexander, Mack, Goetz, Loranty, et al., 2012; C. K. Wang et al., 2001),

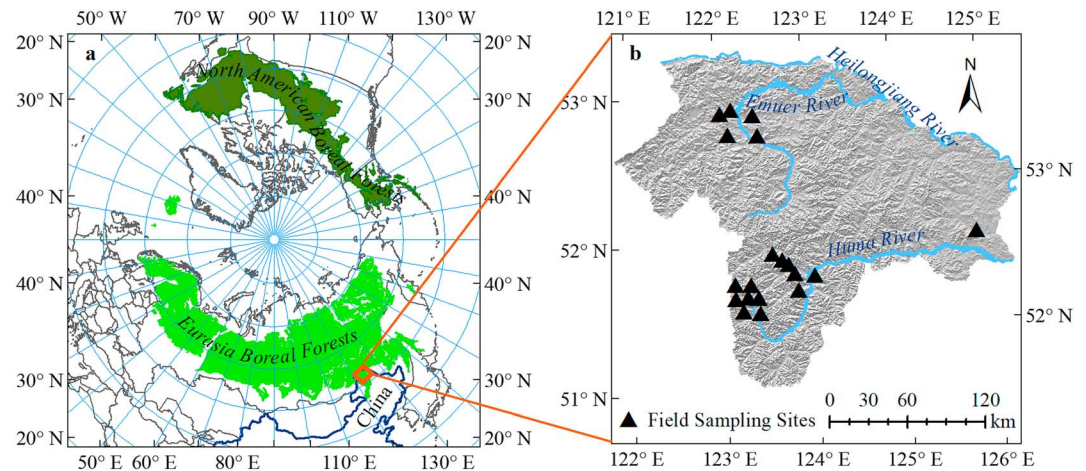


Figure 1. Study area and the field sampling sites (stratified sampling with about 12 plots in each site). The left figure (a) shows the study area which was located on the southern boundary of the eastern Siberian larch forest biome. The right figure (b) shows field study stands represented by solid triangles.

even though over 70% of the world's boreal forests occur in this region (de Groot, Flannigan, et al., 2013). In contrast to North American boreal forests and subalpine ecosystems where evergreen coniferous tree species (e.g., black spruce, *Picea mariana* (Mill.) B.S.P.; lodgepole pine, *Pinus contorta ssp. latifolia*) dominate, nearly half of the C accumulated in Eurasian boreal biome is contained in larch forests (Alexeyev et al., 1995), which are composed of a single deciduous coniferous tree genus (larch, *Larix spp.*) characterized by nonserotinous and the ability to grow on continuous permafrost (Osawa et al., 2010). Eastern Siberian boreal larch forests are dominated by surface fires, while North American boreal forests are dominated by crown fire (de Groot, Cantin, et al., 2013; Flannigan, 2015; Rogers et al., 2015; Turner et al., 2004, 2016). Although some studies have attempted to estimate postfire AC in northeastern Siberia (Alexander, Mack, Goetz, Lorant, et al., 2012; Berner et al., 2012), our current knowledge is limited for Eurasian larch forest ecology and potential susceptibility to changes in fire regimes remains unclear.



Figure 2. Fire-induced tree mortality rate is typically high in boreal larch forests. The panorama (a) shows the landscape of a postfire boreal larch forest, and the inserted picture (b) exhibits the character of larch root system.

Table 1
Summary of Field Methods for Sampling Biomass Pools

Biomass pool	Measured variables	Methodology in each site
Live Trees	DBH	Measured all the trees (DBH \geq 4 cm) in the site and used with allometric equations ^a .
Saplings	BD	Measured all the saplings (DBH < 4 cm) in the site and used with allometric equations by ourselves
<i>Pinus pumila</i>	$D_{0.2}$, D_B , L	Measured all the <i>Pinus pumila</i> in the site and used with allometric equations ^b .
Medium Shrubs	a, b, H , N	The biomass is estimated using allometric equations developed with 20 samples for each species
Dwarf Shrubs	Fresh mass	Three or four samples were oven dried to determine the percentage of dry matter and estimate biomass
Herbs	Fresh mass	Three or four samples oven dry to determine the percentage of dry matter and estimate biomass
Snags	DBH and residual proportion of branch	Measured all the snags in the site and used with allometric equations ^a and subtracted foliage and partial branch.
Fallen Dead Trees	DBH and residual proportion of branch	Measured all the fallen dead trees in the site and used with allometric equations ^a and subtracted foliage and partial branch.
CWD	Midpoint diameter, length, and decay class	Measured all the CWD (DBH \geq 7.6 cm) in the site and the volume multiplied by density of special CWD
Litter Fall	Fresh mass	Samples were collected in three subplots with 1 \times 1 m in main plot, oven dried to determine the percentage of dry matter

Note. All sampling occurred in 4 \times 50 m plots. DBH (cm) is the diameter at breast height (measured at 1.4 m); BD (cm) is basal diameter; $D_{0.2}$ (cm) is the diameter of the creeping stem at 20 cm above the ground; D_B (cm) is the diameter of the top stem at a height just below the base of the lowest living branch; L (cm) is the length of the top stem; a (m) is the major crown axis; b (m) is the minor crown axis; H (m) is the height of the shrub; and N is the number of stems (stems fuse beneath the soil surface). CWD = coarse woody debris.

^aC. K. Wang (2006). ^bKajimoto (1989, 1992).

In this study, we attempt to examine postfire AC dynamics of boreal larch forests in the Great Xing'an Mountains of Eurasia by collecting extensive fire chronosequence data that covered multiple stand age classes ranging from early-successional, midsuccessional, and late-successional stages for up to 200 years after fire, and encompassed a variety of stand densities within each successional stage. The primary objective of this study is to quantify the turning point and recovery time of postfire AC trajectory and its association with stand density along the successional gradient. Our specific questions are as follows:

1. How does the temporal trajectory of LAC compare to DAC following fire?
2. When does C sequestration by regenerating vegetation surpass C loss through coarse woody debris (CWD) decomposition?
3. How does the relationship between stand density and C storage in live trees vary among successional stages?

2. Materials and Methods

2.1. Study Area

Our study focused on a boreal larch forest located in the Great Xing'an Mountains (51°14'N 121°12'E to 53°33'N 125°50'E), Northeastern China, and encompassed about 3.89 \times 10⁶ ha (Figure 1). The study area is characterized by a continental monsoon climate with mean annual air temperature of -2 °C and annual total precipitation mean of 500 mm, both of which were calculated from recorded climate data ranging from 1983 to 2013 (<http://data.cma.cn/data/>). This region is characterized by gentle slopes and valley bottoms and underlain by discontinuous permafrost or seasonally frozen ground (Xu, 1998). The parent rocks in all sites are granite, and the soil is a dark brown forest soil (C. K. Wang et al., 2001; Xu, 1998).

The dominant vegetation in this study area is Dahurian larch (*Larix gmelinii* (Rupr.) Kuzen.) that adapts to cool and moist sites. Other common coniferous species include spruce (*Picea koraiensis* Nakai) and pine (*Pinus sylvestris* Linn. var. *mongolica* Litv). Deciduous broadleaf species include white birch (*Betula platyphylla* Suk.), two aspen species (*Populus davidiana* Dode., and *Populus suaveolens* Fisch.), Mongolian oak (*Quercus mongolica* Fisch. ex Ledeb.), and willow (*Chosenia arbutifolia* (Pall.) A. Skv.; Xu, 1998; Zhou et al., 1991). The understory is mainly composed of shrub species including Siberian dwarf pine (*Pinus pumila* (Pall.) Regel.), ledum (*Ledum palustre* Linn.), linberry (*Vaccinium vitis-idaea* Linn.), rhododendron (*Rhododendron dauricum* Linn.),

Table 2

Allometric Equations for Predicting Dry Biomass (g) of Five Different Aboveground Components of Tree Species and Aboveground Saplings and Shrubs in Larch Forests in the Great Xing'an Mountains

Species	Biomass component	Equations	n	R ²
Larch ^a	Stem	$\log_{10}B = \log_{10}(2.311 + 2.154 \times DBH)$	10	0.96
	Total branch	$\log_{10}B = \log_{10}(-1.593 + 4.340 \times DBH)$	10	0.95
	Total foliage	$\log_{10}B = \log_{10}(-1.851 + 3.934 \times DBH)$	10	0.89
Birch ^a	Stem	$\log_{10}B = \log_{10}(2.141 + 2.278 \times DBH)$	10	0.99
	Total branch	$\log_{10}B = \log_{10}(0.952 + 2.783 \times DBH)$	10	0.96
	Total foliage	$\log_{10}B = \log_{10}(1.176 + 1.942 \times DBH)$	10	0.92
Larch sapling ^c	Stem	$B = 10.84 \times BD^{2.828}$	79	0.99
	Total branch	$B = 7.07 \times BD^{2.955}$	79	0.96
	Total foliage	$B = 7.767 \times BD^{2.564}$	79	0.98
Birch sapling ^c	Stem	$B = 10.74 \times BD^{2.795}$	82	0.98
	Total branch	$B = 2.559 \times BD^{3.403}$	82	0.94
	Total foliage	$B = 10.53 \times BD^{2.243}$	82	0.98
<i>Pinus pumila</i> ^b	Top stem	$B = 0.679 \times (D_{0.2}^2 \times L)^{0.85}$	10	0.99
	New branch	$B = 0.620 \times (D_B^2)^{1.19}$	10	0.94
	Older branch	$B = 4.65 \times (D_B^2)^{1.58}$	10	0.95
	New foliage	$B = 4.70 \times (D_B^2)^{1.04}$	10	0.96
	Older foliage	$B = 11.3 \times (D_B^2)^{1.08}$	10	0.99
<i>Rhododendron</i> ^c	Aboveground biomass	$B = 1408 \times (CA \times H)^2 + 861.3 \times CA \times H + 15.784$	20	0.94
<i>Betula fruticosa</i> ^c	Aboveground biomass	$B = -0.3858 \times (CA \times H \times N)^2 + 53.217 \times CA \times H \times N + 31.907$	18	0.97
<i>Vaccinium uliginosum</i> ^c	Aboveground biomass	$B = 49.974 \times CA \times H \times N + 5.9024$	20	0.82
<i>Ledum palustre</i> ^o	Aboveground biomass	$B = 49.108 \times (CA \times H \times N)^{0.4899}$	20	0.85

Note. B is dry biomass (g); DBH (cm) is the diameter at breast height (measured at 1.4 m); BD (cm) is the basal diameter; D_{0.2} (cm) is the diameter of the creeping stem at 20 cm above the ground; D_B (cm) is the diameter of the top stem at a height just below the base of the lowest living branch; L (cm) is the length of the top stem; CA (m²) is the size of the shrub crown, CA = πab/4, in which a (m) is the major crown axis, and b (m) is the minor crown axis; H (m) is the height of the shrub; and N is the number of stems (stems fuse beneath the soil surface).

^aC. K. Wang (2006). ^bKajimoto (1989, 1992). ^cAuthors' experience.

lespedeza (*Lespedeza bicolor* Turcz.), and dwarf bog birch (*Betula fruticosa* Pall.), and some herbaceous species including willow herb (*Epilobium angustifolium* Linn.), pyrola (*Pyrola* Linn.), and sedge (*Carex appendiculata* (Trautv.) Kukenth) that vary with topographic positions and soil conditions (Xu, 1998; Zhou et al., 1991).

The fire free interval in the Great Xing'an Mountain region historically ranges from 120 to 150 years (Xu et al., 1997). Boreal larch forests in this region tend to experience more surface fires than North American boreal spruce forests and lodgepole pine systems (de Groot, Cantin, et al., 2013; Flannigan, 2015; Rogers et al., 2015; Turner et al., 2004, 2016). The dominant tree species (e.g., black spruce) in North American boreal forests have highly flammable needle foliage and low dense live branches, which act as ladder fuels that help a surface fire to reach the tree crowns and generate a crown fire (de Groot et al., 2009; de Groot, Flannigan, et al., 2013; Flannigan et al., 2016). In contrast, the larch tree species have self-pruning character (Ban et al., 1998). However, although larch is generally regarded as a fire-tolerant species, the mortality rate is high (greater than or equal to 95%, calculated from our unpublished field sampling data) because of its horizontal shallow-distributed root systems (Figure 2; Fang et al., 2015; Kobak et al., 1996).

2.2. Field Sampling

Field sampling was conducted during the summers of 2014 and 2015 in different burned patches with various stand age classes (Figure 1). We compiled a chronosequence of 175 larch plots to examine postfire AC storage dynamics. A chronosequence is predominantly used to study temporal dynamics of ecosystem developments over long time periods (Chen et al., 2013; Clemmensen et al., 2013, 2015; Walker et al., 2010). We sampled naturally regenerated stands with different time since last fire (4, 14, 27, 50, 70, 90, 150, and 200 years) on three topographic positions (south-facing slopes, north-facing slopes, and valley bottoms) using a stratification sampling scheme to control for the differences in site quality in confounding the temporal reconstructions. Stand age was established based on available historical fire occurrence records that have been documented since 1965 for stand age ≤50 years old (Z. H. Liu et al., 2012). For stands >50 years old, stand ages were determined by coring the rings of dominant trees at breast height (1.3 m above the root collar; Hart & Chen, 2008). To minimize edge effects and spatial autocorrelation, all plots were placed at least

Table 3
Carbon Content of Biomass Pools for Larch Forests in the Great Xing'an Mountains

Species	Tissue-specific C content (%)				Mean C content (%)
	Foliage	New branch	Old branch	Stem	
Larch ^a	49.2	50.4	47.9	46.7	46.9
Birch ^a	48.9	49.8	46.5	45.9	46.1
<i>Pinus pumila</i> ^a	56.4	54.5	53.8	52.6	53.2
<i>Rhododendron</i> ^b	--	--	--	--	43.0
<i>Betula Fruticosa</i> ^b	--	--	--	--	40.9
<i>Vaccinium uliginosum</i> ^b	--	--	--	--	42.1
<i>Ledum palustre</i> ^b	--	--	--	--	40.5
<i>Vaccinium vitis-idaea</i> ^b	--	--	--	--	39.9
<i>Lespedeza</i> ^b	--	--	--	--	45.5
<i>Onagraceae</i> ^b	--	--	--	--	40.4
<i>Cyperaceae</i> ^b	--	--	--	--	38.5
<i>Convallaria</i> ^b	--	--	--	--	41.3
<i>Pyrolaceae</i> ^b	--	--	--	--	37.3
<i>Campanulaceae</i> ^b	--	--	--	--	37.1

Note. "--" represents no data.

^aZhang et al. (2009).

^bJiao (2006).

500 m away from roads or trails, and the distance between each plot location was at least 300 m. In order to cover the full range of variations in each category, a minimum of four plots were selected and measured in each combination of stand age cohort and topographical position classes.

The default plot size was a 4 × 50 m belt transect laid out in the stand with the center of the plot at a random location (Kashian et al., 2004). The plot size was objectively increased to 10 × 50 m in certain plots where tree density was low in order to capture ≥50 trees in a plot (Harvey et al., 2016b). This configuration was most ecologically appropriate for reducing the influence of spatial heterogeneities of patches with different tree densities in the field. Along each belt transect, we measured the following parameters: diameter at breast height (DBH) of all live trees (DBH ≥ 4 cm), snags, and fallen dead trees; basal diameter (BD) of saplings (DBH < 4 cm); midpoint diameter, length, and decay class of CWD (≥7.6 cm; Kang, 2012; Li, 2013); among many others (detailed parameters are listed in Table 1). It should be noted that the biomass of shrub species *P. pumila* was also measured in the belt transect due to its procumbent and intricately ramified stems around the surface (Kajimoto, 1992).

Four subplots (2 × 2 m) were established with roughly equidistant spacing along the belt transect to estimate the biomass of tall shrubs (height ≥ 0.3 m, except *P. pumila* as its biomass was measured in the plot for trees). Major and minor crown axes, height of the shrub, and the number of stems were recorded for estimating the biomass of tall shrubs in these plots. A secondary subplot of 1 × 1 m was arranged in the center of each larger subplot to estimate the biomass of dwarf shrubs (height < 0.3 m) and herbs, the dry mass of fine woody debris (FWD), and litter. Detailed sampling methods and measured parameters are described in the following paragraphs and listed in Table 1.

Table 4
Wood Density and C Content of Coarse Woody Debris and Stumps for Larch and Birch in the Great Xing'an Mountains

Decay class	Larch		Birch	
	Density (g/cm ³) ^a	C (%) ^b	Density (g/cm ³) ^a	C (%) ^b
I	0.58	47.28	0.50	47.03
II	0.46	45.54	0.41	45.38
III	0.34	44.54	0.35	42.14
IV	0.24	47.02	0.16	43.67
V	0.16	44.65	0.08	39.69

^aKang (2012). ^bLi (2013).

2.3. Allometric Equations

Aboveground biomass of trees including larch and birch was calculated using allometric equations (Table 2) developed specifically for this study area (C. K. Wang, 2006). For every tree (DBH ≥ 4 cm) within the plot, the species identity and measured DBH were recorded and used to calculate the biomass of each tree components (foliage, branch, and stem using the allometric equations). Because allometric equations for saplings were not readily available in this region, we developed our own equations to estimate aboveground biomass of saplings (larch and birch). Approximately 80 saplings of each species were randomly sampled in three topographic positions (south-facing slopes, north-facing slopes,

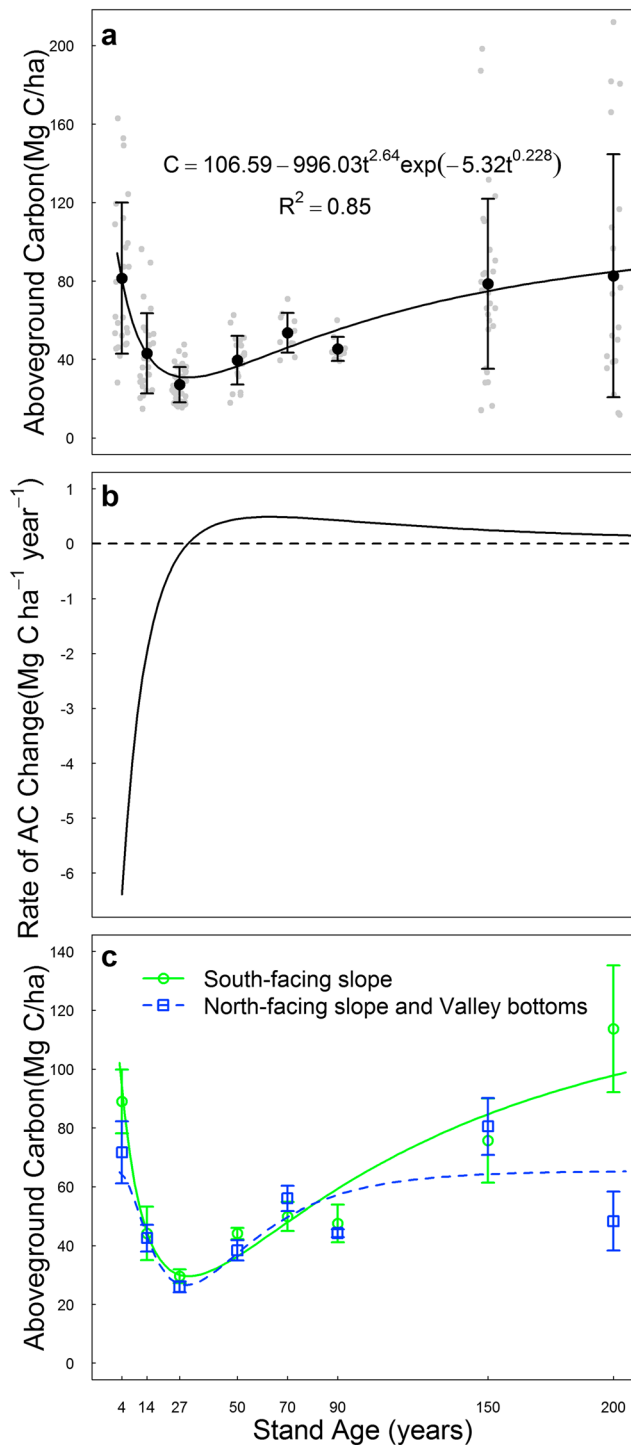


Figure 3. The dynamic patterns of total AC. (a) Changes in AC (Mg C/ha) with years since fire. Values are means \pm standard deviation, the gray points are field sampling data. (b) The rate of aboveground carbon change was a function of stand age (time since fire). The curves in the figure represent the rate of AC through time estimated from the first derivative of the gamma functions described in the text. (c) The dynamic patterns of AC in different topographic position. Values are means \pm standard deviation. South-facing slopes $C = 131.69 - 1574.92t^{2.46} \exp(-5.24t^{0.221})$, $R^2 = 0.88$; valley bottoms and north-facing slopes $C = 65.38 - 2.01t^{6.37} \exp(-5.82t^{0.343})$, $R^2 = 0.15$. AC = aboveground carbon.

and valley bottoms), and BD was measured. The fresh foliage, branches, and stems were divided and weighed separately, and then approximately 300 g of fresh mass were randomly sampled from each component and taken in labeled muslin bags to the laboratory for estimating the percentage of dry matter (equation (1)). The dry matter was calculated through multiplying the fresh matter of each component by its percentage of dry matter. Allometric equations for aboveground biomass of saplings were developed using BD and dry weight of the saplings (Table 2).

$$P_d = \frac{W_d}{W_f} \times 100\%, \quad (1)$$

where P_d is the percentage of dry matter, W_d is the weight of dried samples, W_f is the weight of fresh samples.

Allometric equations for shrubs, such as *rhododendron*, *betulaceae*, *Vaccinium uliginosum*, and *Ledum palustre*, were developed using our field survey data in this region. Over 20 samples of each species were randomly collected; for these samples, shrub height, number of stems, and major and minor crown axes were measured. The fresh mass was weighed and oven-dried to calculate the percentage of dry matter (equation (1)). The allometric equations for biomass of the shrubs were developed based on dry weight of shrub and the characteristics previously measured (Table 2).

We used different approaches to estimate the biomass of tall shrubs, dwarf shrubs, and herbs. Tall shrub biomass was estimated using either the allometric equations developed by Kajimoto (1989) or the equations we developed (Table 2). Parameters of equations for estimating the biomass of *P. pumila* include $D_{0.2}$ (the diameter of the creeping stem at 20 cm above the ground), D_B (the diameter of the top stem at a height just below the base of the lowest living branch), and L (the length of the top stem). These parameters were measured for each *P. pumila* in the plot (Table 1). For other tall shrubs, the corresponding parameters were measured in three or four 2 \times 2 m subplots, and the biomass was calculated using corresponding allometric equations (Table 2). The dwarf shrubs and herbs were destructively harvested in randomly distributed 1 \times 1 m secondary subplots inside each subplot.

2.4. AC Estimation

AC storage was the sum of LAC and DAC. LAC was contributed by live trees (DBH \geq 4 cm at 1.4 m), saplings (DBH < 4 cm), and understory; DAC was obtained from the sum of snags, dead fallen trees previously rooted in the plot, CWD (diameter \geq 7.6 cm), FWD (diameter < 7.6 cm), and litter (Table 1). Each C pool was estimated by multiplying the component biomass with the corresponding C content which was obtained from Zhang et al. (2009) and Jiao (2006; details listed in Table 3).

Snags refer to dead trunks that leaned $< 45^\circ$ with or without branches (Bond-Lamberty et al., 2002). According to the branches retained, they could be classified into four categories: (1) $> 75\%$, (2) 50–75%, (3) 25–50%, and (4) $< 25\%$ branches retained. DBH was measured for all snags in the plots and was used to estimate the biomass of tree components via allometric equations published (to estimate live tree biomass) by C. K. Wang (2006). Once the trees were killed by fire and transformed to snags, they began to decompose. A negative exponential function (equation (2))



Figure 4. Changes in the proportion of live and dead AC in the total AC throughout forest stand developmental stages. AC = aboveground carbon.

was fit to describe heterotrophic respiration in snags following the equation from Janisch and Harmon (2002) and Freschet et al. (2012):

$$D_t = D_0(e^{-kt}), \quad (2)$$

where D_t is legacy snag C storage at time t after fire, D_0 is prefire C storage of live trees excluding leaves and partial branches that were burned out or fell down, and k is an empirically derived heterotrophic respiration rate constant with $k = 0.03$ for conifer trees and $k = 0.05$ for broadleaf trees, respectively (Hogg & Michaelian, 2015; Russell et al., 2014). This equation was used to estimate the retained C storage in snags at any time t after fire.

Fallen dead trees were defined as all dead trees lying on the ground or standing (with a zenith angle $\geq 45^\circ$), which exhibited the same characteristics as snags except exposed root system. C storage in fallen dead trees was estimated in the same way as snags, and the stumps and root systems were assumed as portions of AC storage.

CWD was defined as downed tree boles at least 0.5 m in length and ≥ 7.6 cm in diameter at the middle. Within each plot, the measured midpoint diameter, measured length, species identity, and decay class of all CWD were recorded. The decay class was assigned into five categories and ranked from 1 (least decayed) to 5 (most decayed; Gough et al., 2007). CWD was assumed to be cylindrical, and the volume was calculated according to equation (3):

$$V = \pi D^2 L / 4, \quad (3)$$

where V was the volume, D was the midpoint diameter, and L was length of CWD. The CWD volume was converted to biomass using CWD density values (Table 4) developed by Kang (2012), and dry biomass was multiplied by C content (Table 4) of CWD to convert into C mass (Li, 2013).

Litter fall included FWD (diameter < 7.6 cm), dead grass, and leaves, which still retained their original shape and were visually distinguishable. The decomposed litter material was considered part of the soil C pool, therefore, left out of the AC pool. The FWD, grasses, and leaves were collected and weighed, respectively, in 1×1 m secondary subplots randomly located in each subplot. C content was assumed to compose 45% of the mass of dead wood, and 42% of mass for dead grasses and leaves (Li, 2013).

2.5. Data Analysis

For consistency, all C pools were scaled up to Mg C per hectare. Mean and standard deviation were calculated for each AC component and total AC in different age cohorts. A chronosequence was also developed to examine the pattern of postfire AC storage dynamics in boreal larch forests. Linear and nonlinear regression analyses were used to describe the patterns in LAC, DAC, and AC trajectory. For each C pool, mean C mass was calculated at each stand age, and these data were fitted to a linear function, a Chapman-Richards function (equation (4)), which produces a sigmoidal curve (Taylor et al., 2007), a gamma function (equation (5)), which produces a U-shaped curve (Covington, 1981; White et al., 2004), and a negative exponential function (equation (6)), which produces an inverse J-shaped curve (Rothstein et al., 2004). The best fit was determined as the function with the smallest mean square error (Yang et al., 2011; Zak et al., 1990).

$$C = a[1 - \exp(-bT)]^c, \quad (4)$$

$$C = aT^b \exp(cT^d) + e, \quad (5)$$

$$C = a \exp(-bT) + c, \quad (6)$$

where C is C mass (Mg C per hectare); T is stand age (years); a , b , c , d , and e are statistical coefficients.

To estimate the turning point of postfire AC trajectory, we computed first and second derivatives of its fitted function. The turning point was determined as the local maximum or minimum of the function at which first derivative equals to zero and second derivative is negative or positive, respectively. The resilience time was

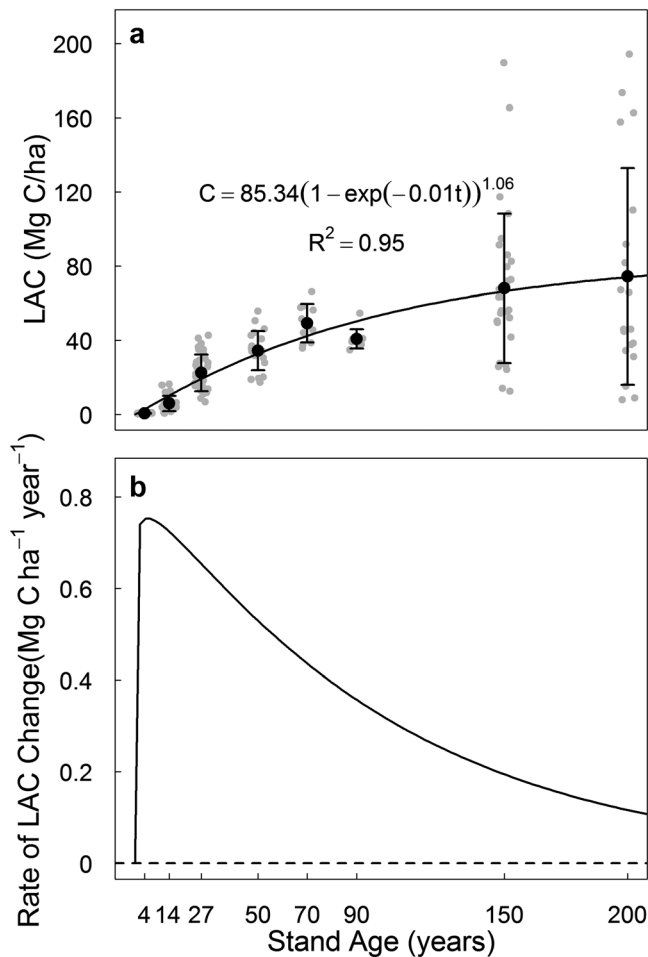


Figure 5. The dynamic patterns of LAC. (a) Changes in LAC (Mg C/ha) with years since fire. Values are means \pm standard deviation, the gray points are field sampling data. (b) The rate of LAC change was a function of stand age (time since fire). The curves in the figure represent the rate of LAC through time estimated from the first derivative of the Chapman-Richards functions described in the text. LAC = live aboveground carbon.

estimated as the time needed for the postfire AC mass reaching $>80\%$ of the reference old-growth (200 years old) larch forest stand (C. K. Wang et al., 2003; Xu, 1998).

We computed the Pearson correlation coefficient between stand tree density and LTAC, LAC, as well as AC for each stand age class. Because both stand tree density and C pools would change with stand age, in order to examine the general relationship between C pools and stand tree density across all different stand age classes, we normalized C pools into z-score at the stand age cohort level and computed relative stand tree density for each age class as tree density/maximum tree density, where maximum tree density is determined as the maximum tree density at each specific age cohort class (Kashian et al., 2013). We then fitted the normalized C pool data with three linear regression models with one model considering relative stand density alone, one considering the additive effects of both relative stand density and stand age, and one considering the interactive effects. The three models were then compared with an ANOVA Type-I test. All statistical analyses were performed in Origin 8.0 software and R (R Development Core Team, 2017).

3. Results

AC was delineated by a skewed U-shaped curve with an initially rapid decline, followed by a gradual increase with time since last fire (Figure 3a). The entire AC chronosequence was best described by the gamma function that explained 85% of variation. The turning point of the postfire AC trajectory was estimated based on the first derivative of the parameterized gamma function, which essentially described the annual rate of AC accumulation (Figure 3b). The net change of AC was negative in the first two decades and became positive when reaching the turning point at year 30. The rate continued to increase until reaching the maximum of the $0.49 \text{ Mg C} \cdot \text{ha}^{-1} \cdot \text{year}^{-1}$ at year 65 (Figure 3b). Although AC continued to increase at the late successional stage, the annual net gain leveled approaching $0.25 \text{ Mg C} \cdot \text{ha}^{-1} \cdot \text{year}^{-1}$ at year 150. It took about 120 and 150 years for the postfire AC to achieve 80% and 90% of the level of unburned stands 200 years old, respectively.

AC declined from $81.40 \pm 38.47 \text{ Mg C/ha}$ (Mean \pm Standard deviation) 4 years postfire to an estimated minimum of $27.08 \pm 9.05 \text{ Mg C/ha}$ 27 years postfire, and then increased across the chronosequence, approaching an estimated maximum of $82.71 \pm 61.99 \text{ Mg C/ha}$ at 200 years after a fire (Figure 3a). This trend of AC temporal dynamics was consistent in different topographic positions, with south-facing slopes having generally higher AC than north-facing slopes and valley bottoms (Figure 3c). In addition, the decline of AC during the early successional stages and the subsequent increase were faster in south-facing slopes than north-facing slopes and valley bottoms (Figure 3c).

The relative dominance of LAC and DAC shifted along the chronosequence. The DAC comprised up to 99% and 86% of AC (81.40 ± 38.47 and $43.02 \pm 20.54 \text{ Mg C/ha}$) in stands at 4 and 14 years after fire, respectively; the LAC gradually recovered and became the dominant form ($>80\%$) of AC within three decades after fire (Figure 4).

Postfire dynamics of LAC appeared in a sigmoidal pattern (Figure 5a) with slow accumulation during the establishment phase (ca. first 5 years), a period of rapid accumulation between 5 to 20 years, and then a decline in the rate of accumulation (Figure 5b). Postfire LAC increased from $0.67 \pm 0.26 \text{ Mg C/ha}$ at stand age 4 years to $74.54 \pm 58.44 \text{ Mg C/ha}$ at stand age 200 years across the chronosequence. Among all the four functions fitted to the LAC chronosequence data, the Chapman-Richards function had the least mean square error (mean square error = 22.09) and highest R^2 (0.95; Figure 5a), which indicated a logistic growth.

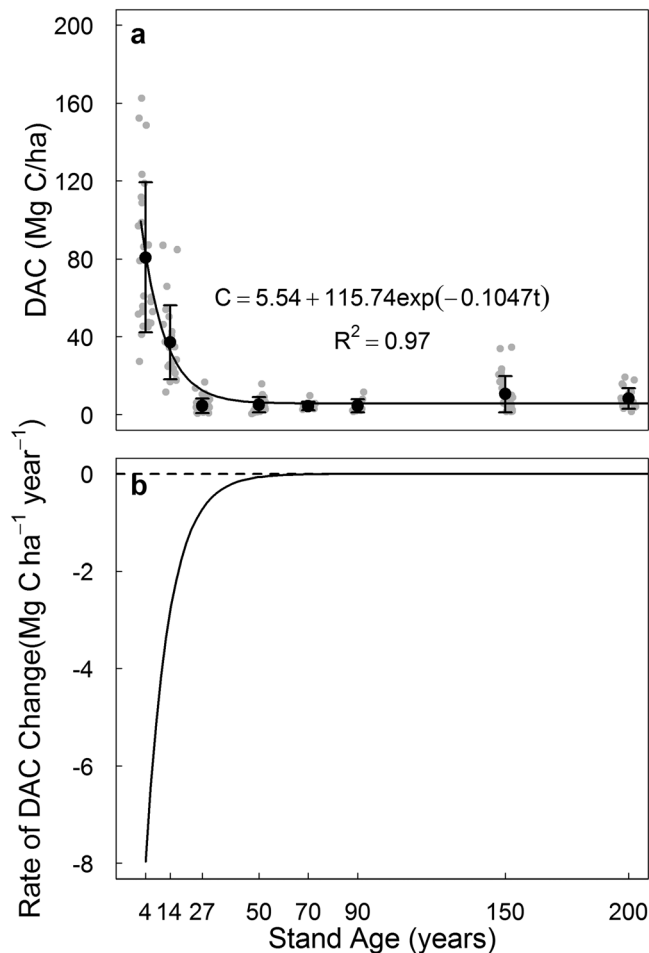


Figure 6. The dynamic patterns of DAC. (a) Changes in DAC (Mg C/ha) with years since fire. Values are means \pm standard deviation, the gray points are field sampling data. (b) The rate of DAC change was a function of stand age (time since fire). The curves in the figure represent the rate of DAC through time estimated from the first derivative of the negative exponential functions described in the text. DAC = dead aboveground carbon.

Herbaceous plants and shrubs dominated the live vegetation C pool at stand age of 4 years, but their relative dominance began to decline as stand age increased (Figure S1).

In contrast, DAC sharply decreased during the early postfire successional stage, and then slowly increased (Figures 6a and 6b). DAC dropped from an estimated maximum of 80.73 ± 38.57 Mg C/ha in the larch forest stands within 4 years after fire to an estimated minimum of 4.35 ± 2.11 Mg C/ha by 70 years after fire, and then increased to 10.45 ± 9.21 Mg C/ha in the stands at 150 years after fire. However, it was the negative exponential decay function that fitted the DAC chronosequence data the best (mean square error = 120, $R^2 = 0.97$; Figure 6a).

The correlation analysis showed that LTAC and stand density had a positive association for each of the stand age class across the entire successional gradient (Table 5 and Figure 7), except for stand age 4 years in which very few seedlings have reached tree (DBH ≥ 4 cm) status. The correlation was the greatest at stand age 14 years ($r = 0.97$) and the least at stand age 70 years ($r = 0.44$). The correlation between LTAC and stand density was statistically significant for most of the stand age classes, except for stand age 70 and 90 years ($p = 0.20$ and 0.11 , respectively). The correlation between LAC and stand density remained positive with slightly smaller r values, and the correlation between total AC and stand density became even weaker with more stand age classes (stand age 50, 70, 90 years) exhibiting a statistically insignificant relationship (Table 5). However, when evaluating the relationship between AC pools and stand density in relative terms (i.e., normalized C and density within each stand age class) for the pooled data set, we found a significant positive relationship between the scaled LTAC, LAC, and AC with the relative stand density (Figure 8). The ANOVA Type-I test did not find a significant interaction effect ($F = 0.70$, $p = 0.65$) of stand density and stand age on LTAC (all variables were normalized), but did show a significant main effect ($F = 46.04$, $p < 0.01$) of relative stand density and a significant additive effect ($F = 4.41$, $p < 0.01$) of stand age class after controlling the relative stand density (Table 6).

4. Discussion

4.1. Postfire AC Dynamics

Our chronosequence AC data showed that the postfire AC pool of Eurasian boreal larch stands initially declined, then increased rapidly, and finally reached a stable condition. This overall AC trajectory is also found in other fire-prone forest ecosystems. For example, Rothstein et al. (2004) observed an initial decrease in total C storage in jack pine forests in Michigan, followed by an increase as stands develop along 72-year chronosequence. Seedre et al. (2014) also depicted a similar pattern in jack pine forest of central Canada over a 27-year chronosequence following fire.

The results of nonlinear regression analysis showed that the AC pools in stands along this chronosequence remained as net C sources to the atmosphere until approximately 30 years after fire (Figure 3a), losing about an average of $1.94 \text{ Mg C} \cdot \text{ha}^{-1} \cdot \text{year}^{-1}$ over this period (Figure 3b).

Our results showed that the LAC increased following a sigmoidal pattern over time (Figure 5a), which was similar to studies in other regions (Bradford et al., 2008; Law et al., 2003; Williams et al., 2012). During the early postfire successional stage, herbaceous vegetation and shrubs recovered quickly and dominated LAC pool, but their magnitude was small. LAC began to increase rapidly when tree seedlings established and dominated the AC pool after 6–8 years since last fire, indicating a similar trend to other

Table 5
The Parameters of Pearson's Correlation Between AC and Stand Density

Stand age	LTAC		LAC		AC	
	r	p value	r	p value	r	p value
14	0.97	<0.01	0.95	<0.01	0.39	0.05
27	0.46	<0.01	0.45	0.01	0.40	0.02
50	0.49	0.03	0.50	0.02	0.43	0.06
70	0.44	0.20	0.42	0.23	0.33	0.36
90	0.54	0.11	0.54	0.11	0.22	0.54
150	0.50	<0.01	0.51	<0.01	0.48	<0.01
200	0.49	0.03	0.49	0.03	0.50	0.03

Note. AC = aboveground carbon; LTAC = live trees AC; LAC = live AC.

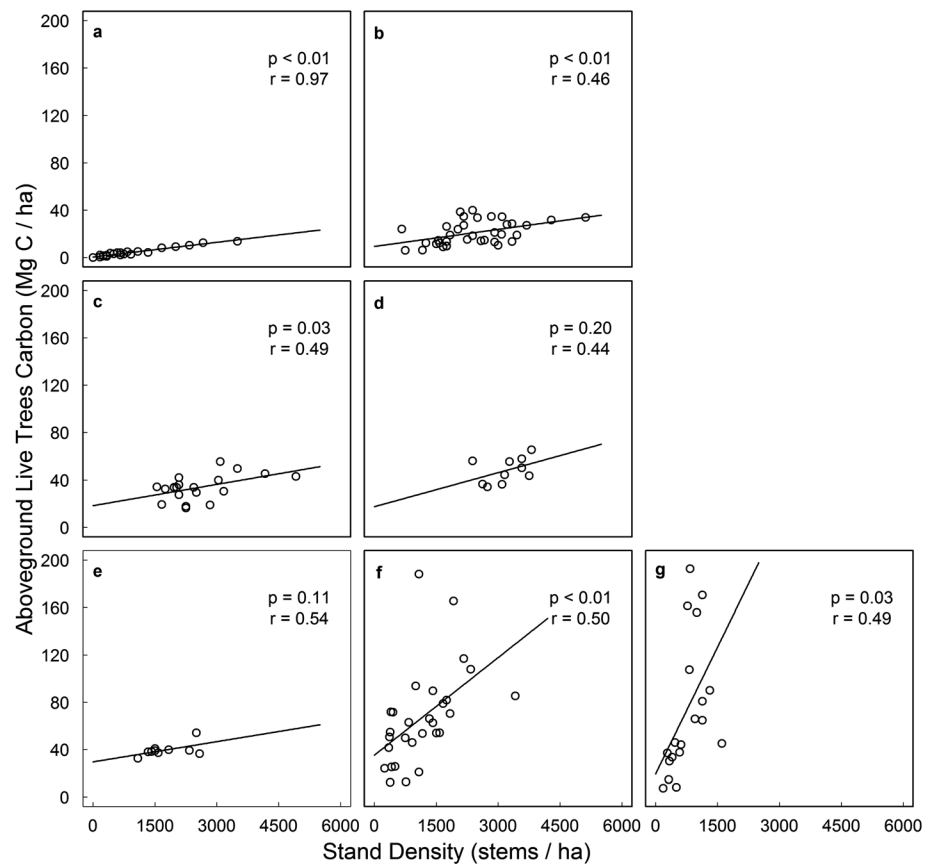


Figure 7. The relationship between live trees aboveground carbon and stand density in various stand ages: (a) 14, (b) 27, (c) 50, (d) 70, (e) 90, (f) 150, and (g) 200 years.

studies (e.g., Harvey et al., 2016b; Johnstone & Kasischke, 2005). The accumulation rate of LAC declined due to resource limitation when the canopy closed (Figure 5b).

DAC, the other component of AC, decreased sharply during the early postfire successional stage (<30 years), and then increased slowly (Figures 6a and 6b). Similar patterns had been reported in previous studies (Alexander, Mack, Goetz, Loranty, et al., 2012; Rothstein et al., 2004). Brassard and Chen (2007) indicated that the CWD C pool followed a U-shaped trend with increased stand age in North American boreal forests. The initial high CWD C, which originated from fire legacies, could influence short- and long-term C cycle (Gough et al., 2007; Manies et al., 2005). C emission into the atmosphere is generally considered to be a dominant pathway of DAC loss (Chapin et al., 2011; S. G. Liu et al., 2011). However, C moving into the soil pool is another important pathway in these systems where decomposition is slow (S. G. Liu et al., 2011). The dissolved organic and inorganic C originated from dead wood and pyrogenic C are transferred into the soil and other C storage pools through leaching, lateral fluxes, and particulate C (Bird et al., 2015; Chapin et al., 2006; Santin et al., 2015). Therefore, DAC acted as a C source to other components of the ecosystem. Further studies are needed to assess whether the entire ecosystem is a C source or sink.

In this study, we employed a stratified sampling scheme for the purpose to represent the full spectrum of AC dynamics across different topographic positions. The topography exerts strong influences on spatial variability of C storage (Cai et al., 2018), but the general trend of AC dynamics was similar across different topographic positions. There were some variations in the recovery rate among topographic positions due to its regulating effects on microclimatic conditions such as light, water, and heat condition. The mature and old-growth forest in south-facing slopes tend to grow better and faster because solar radiation is greater in south-facing slopes than north-facing slopes and valley bottoms in the northern hemisphere. Consequently, forests in south-facing slopes tend to sequester more AC and have a faster AC

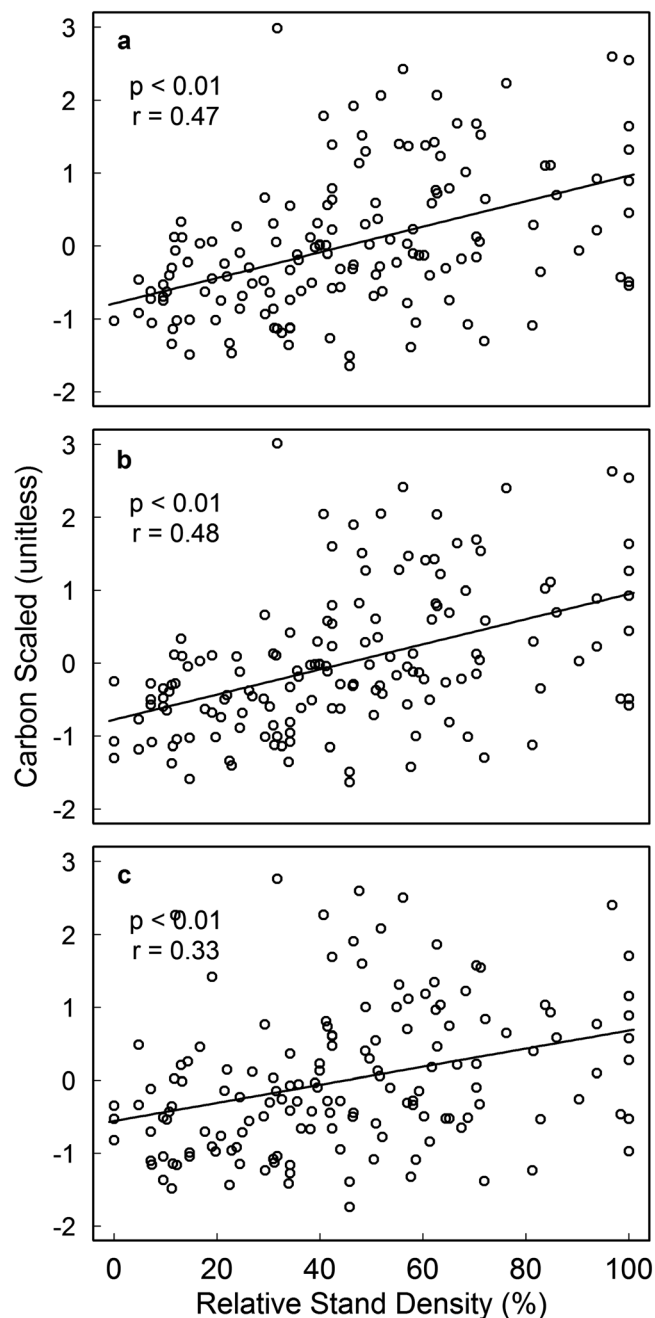


Figure 8. The relationship between carbon that is scaled into a z-score and relative stand density that is normalized as the fraction of absolute stand density to the maximum of stand density of its specific stand age class across all successional stages for the following aboveground carbon pool types: (a) live trees aboveground carbon scaled, (b) live aboveground carbon scaled, and (c) total aboveground carbon scaled.

tree size is relatively small as early postfire soil resources and growth space were rich (Kong et al., 2015), and during the late-successional stage, when the landscapes were dominated by fewer but larger trees. However, such positive relationships were found not significant during the midsuccessional stage. This could be attributed to the variation in site quality, which may play a stronger role in determining the variation of LTAC than density during this particular successional stage.

accumulation rate during mid- and late-successional stages. However, postfire forests in south-facing slopes also tend to lose more AC during the early successional stages due to higher decomposition rate of dead trees in warmer sites (Figure 3c).

4.2. AC Storage and Sequestration in Response to Changing Climate and Fire Regime

Postfire AC dynamics indicated that AC could recover to prefire levels under the contemporary fire free interval (120–150 years; Osawa et al., 2010; Zhou et al., 1991). This result was consistent with other studies (greater than or equal to 100 years) in Siberian larch forests, but the old-growth forest in this study area stored more C than other similar stands (40–50 Mg C/ha; Alexander, Mack, Goetz, Lorant, et al., 2012; Osawa et al., 2010). This discrepancy may be related to spatial variations of the growth rate and potential AC stock, which tends to decrease on a south-to-north gradient, varied along a latitudinal gradient in boreal larch forests due to hydrothermal conditions (Usoltsev et al., 2002).

Recent climate warming has enhanced AC sequestration in northern high latitudes (Barichivich et al., 2013; Berner et al., 2013). Globally, net primary production (NPP) increased by 6.17% (3.42 Pg C) between 1982 and 1999, 38% of which was contributed from boreal forests (Nemani et al., 2003). However, frequent and severe fire disturbances under climate warming can potentially offset the direct positive effects of climate change on NPP (Dale et al., 2001; Flannigan et al., 2005; Girardin et al., 2009; Stephens et al., 2014). Fire frequency and burn size have already been observed to increase in boreal forests (Goetz et al., 2007; Riaño et al., 2007; Stephens et al., 2014) and are critical for predicting possible changes in C storage. Flannigan et al. (2009) suggested that increases in fire frequency may have converted boreal forest into a C source in Canada. In the Great Xing’an Mountains, fire regime models have predicted that climate warming could increase fire frequency by 30% to 230% by the end of 21st century (Z. H. Liu et al., 2012), which would greatly shorten the fire free interval (historical mean fire free interval of 120–150 years; Xu et al., 1997). Repeated disturbances would cut short C recovery time and reduce C recovery rate through limiting seed and propagule availability (Harvey et al., 2016a; Jasinski & Payette, 2005; Johnstone & Chapin, 2006). This would delay AC storage recovery, reduce resilience of the boreal forest ecosystem, increase the sensitivity of the ecosystem C balance to climate warming, and possibly reduce to the total C storage capacity (e.g., Seedre et al., 2014; Stephens et al., 2014).

4.3. Relationship Between AC and Stand Density

Our results showed a positive relationship between LTAC and stand density over the entire range of successional stages. This pattern was congruent with the prevalent relationship seen in boreal forests (Alexander, Mack, Goetz, Beck, et al., 2012; Kashian et al., 2006). AC in live trees increased with stand density during the early-successional stage, when the variability of

Table 6
ANOVA Type-I Test of Effects of Relative Stand Density, Stand Age, and Their Interaction on the Scaled Aboveground Live Trees Carbon

	DF	Sum Sq.	F value	p value
Density	1	30.95	46.04	<0.01
Ages	6	17.79	4.41	<0.01
Density:Ages	6	2.83	0.70	0.65
Residuals	136	91.43		

The period of forest stand development that processes canopy closure, stand initiation, is normally the shortest phase in duration (Oliver & Larson, 1996). Although the relationship between high density and high biomass stands could be maintained before canopy closure, high site quality stands may proceed through phases of stand development more rapidly than low productivity sites. For a given age, higher quality sites would have lower densities, larger individual trees, and more live biomass than stands with lower site quality. Therefore, the relationship between live biomass and density within a single successional stage may be compli-

cated by the fact that multiple stand development phases could be attained by the same stand age class, which is probably most conspicuous during the midsuccessional stage.

The standard deviations of standardized AC were quite large during the early- and late-successional stages, while small in the midsuccession (Figure 3). The standard deviation of standardized AC at plots 4 years after fire was high because of the large of variation in DAC, which is attributed to spatial heterogeneity of fire severity and prefire stand structure (Cai & Yang, 2016). The standard deviation at stand age class of 150 and 200 years was also high because these stands have or closely reached to old-growth stage, in which a small variation of tree density would imply a large variation of LAC as one single large 150- or 200-year old larch tree would possess a large quantity of biomass. The variation of LAC in the old-growth stage was determined by the heterogeneity of site quality and biotic interactions (Osawa et al., 2010).

The positive relationship between relative stand density and scaled LTAC can be extended to scaled LAC and AC over the entire range of successional stages (Figure 8). The ANOVA analysis showed that relative stand density and stand age have additive effects on scaled AC. Previous studies have found that early postfire stand density in this region is mainly driven by fire severity (Cai et al., 2013) with patches of low burn severity having high seedling densities. This suggests that spatial heterogeneity in fire severity and resulting regeneration patterns could affect forest C storage variations well into the later phases of stand development.

Predicted increases in fire frequency could exert a positive feedback on climate warming by causing more stands to be replaced by young forests with less C storage. The relationship between shorter fire return interval and fire severity is complex and differs by biome/ecoregion. Some studies have shown that in stands where shorter return interval leads into lower fire severity and consequently higher stand density (Holland et al., 2017; Murphy et al., 2015; Pellegrini et al., 2017). Many forests actually show the opposite trend, where shorter return intervals increase fire severity (Camac et al., 2017; Harris et al., 2016; Taylor et al., 2014; Tepley et al., 2016). Our study area located in the boreal forests accords with the former case, because fuel load reductions may result from shorter fire return intervals in this forest type (Chang et al., 2008; de Groot, Flannigan, et al., 2013). Such self-regulation of the fire regime could contribute greatly to the overall forest resilience in a global change context.

Acknowledgments

This work was funded by the National Key R & D Program of China (2016YFA0600804), National Natural Science Foundation of China (31500387, 41222004, & 41501200), Open Project Program of Key Laboratory of Environment Change and Resources Use in Beibu Gulf (Guangxi Teachers Education University), Ministry of Education (GTEU-KLXTJJ-201718, GTEU-KLXTJJ-201720). We acknowledge Huzhong Forestry Bureau and Huzhong Natural Reserve for the help in field investigations. We also acknowledge China Meteorological Data Sharing Service System (<http://data.cma.cn/data/>) for providing the meteorological data, and thanks for Geospatial Data Cloud (<http://www.gscloud.cn/>) for offering freely digital elevation model (DEM). All data used in this study are available in the supporting information (Data Set S1).

5. Conclusions

The AC pool is an important component of ecosystem C, and understanding postfire AC dynamics is critical for predicting the possible feedbacks of this biome to climate warming. The AC pool could be a C source to the atmosphere for several decades following fire disturbances; and it may take more than a century for the AC to recover 80% of that in old-growth boreal larch forests in the Northeast of China. Increases in fire frequency due to climate change and human activities will shorten the fire free interval and increase C emission, which may significantly influence the regional C budget. Stand density was considered as a positive factor on AC accumulation following wildfire. AC was determined by the combined influence of stand density and tree size, but there was a negative correlation between them. Although stand density was proved to be a key factor regulating postfire AC in live trees during early- and late-successional stages, the effects may be counteracted by variation in tree size due to site productivity in other successional stages.

References

- Alexander, H. D., & Mack, M. C. (2015). A canopy shift in interior Alaskan boreal forests: Consequences for above- and belowground carbon and nitrogen pools during post-fire succession. *Ecosystems*, 19(1), 98–114. <https://doi.org/10.1007/s10021-015-9920-7>
- Alexander, H. D., Mack, M. C., Goetz, S., Beck, P. S. A., & Belshe, E. F. (2012). Implications of increased deciduous cover on stand structure and aboveground carbon pools of Alaskan boreal forests. *Ecosphere*, 3(5), 1–21. <https://doi.org/10.1890/ES11-00364.1>

- Alexander, H. D., Mack, M. C., Goetz, S., Loranty, M. M., Beck, P. S. A., Earl, K., et al. (2012). Carbon accumulation patterns during post-fire succession in cajander larch (*Larix cajanderi*) forests of Siberia. *Ecosystems*, *15*(7), 1065–1082. <https://doi.org/10.1007/s10021-012-9567-6>
- Alexeyev, V., Birdsey, R., Stakanov, V., & Korotkov, I. (1995). Carbon in vegetation of Russian forests: Methods to estimate storage and geographical-distribution. *Water, Air, and Soil Pollution*, *82*, 271–282. <https://doi.org/10.1007/BF01182840>
- Amiro, B. D., Barr, A. G., Barr, J. G., Black, T. A., Bracho, R., Brown, M., et al. (2010). Ecosystem carbon dioxide fluxes after disturbance in forests of North America. *Journal of Geophysical Research*, *115*, G00K02. <https://doi.org/10.1029/2010JG001390>
- Amiro, B. D., Orchansky, A. L., Barr, A. G., Black, T. A., Chambers, S. D., Chapin III, F. S., et al. (2006). The effect of post-fire stand age on the boreal forest energy balance. *Agricultural and Forest Meteorology*, *140*, 41–50. <https://doi.org/10.1016/j.agrformet.2006.02.014>
- Ban, Y., Xu, H. C., Bergeron, Y., & Kneeshaw, D. D. (1998). Gap regeneration of shade-intolerant *Larix gmelini* in old-growth boreal forests of northeastern China. *Journal of Vegetation Science*, *9*(4), 529–536. <https://doi.org/10.2307/3237268>
- Barichivich, J., Briffa, K. R., Myneni, R. B., Osborn, T. J., Melvin, T. M., Ciais, P., et al. (2013). Large-scale variations in the vegetation growing season and annual cycle of atmospheric CO₂ at high northern latitudes from 1950 to 2011. *Global Change Biology*, *19*(10), 3167–3183. <https://doi.org/10.1111/gcb.12283>
- Berner, L. T., Beck, P. S., Bunn, A. G., & Goetz, S. J. (2013). Plant response to climate change along the forest-tundra ecotone in northeastern Siberia. *Global Change Biology*, *19*(11), 3449–3462. <https://doi.org/10.1111/gcb.12304>
- Berner, L. T., Beck, P. S. A., Loranty, M. M., Alexander, H. D., Mack, M. C., & Goetz, S. J. (2012). Cajander larch (*Larix cajanderi*) biomass distribution, fire regime and post-fire recovery in northeastern Siberia. *Biogeosciences*, *9*(10), 3943–3959. <https://doi.org/10.5194/bg-9-3943-2012>
- Bird, M. I., Wynn, J. G., Saiz, G., Wurster, C. M., & Mcbeath, A. (2015). The pyrogenic carbon cycle. *Annual Review of Earth and Planetary Sciences*, *43*(1), 273–298. <https://doi.org/10.1146/annurev-earth-060614-105038>
- Bond-Lamberty, B., Wang, C. K., & Gower, S. T. (2002). Annual carbon flux from woody debris for a boreal black spruce fire chronosequence. *Journal of Geophysical Research*, *107*(D23), WFX 1-1. <https://doi.org/10.1029/2001JD000839>
- Bradford, J. B., Birdsey, R. A., Joyce, L. A., & Ryan, M. G. (2008). Tree age, disturbance history, and carbon stocks and fluxes in subalpine Rocky Mountain forests. *Global Change Biology*, *14*(12), 2882–2897. <https://doi.org/10.1111/j.1365-2486.2008.01686.x>
- Brassard, B. W., & Chen, H. Y. H. (2007). Stand structural dynamics of North American boreal forests. *Critical Reviews in Plant Sciences*, *25*(2), 115–137. <https://doi.org/10.1080/07352680500348857>
- Cai, W. H., & Yang, J. (2016). High-severity fire reduces early successional boreal larch forest aboveground productivity by shifting stand density in north-eastern China. *International Journal of Wildland Fire*, *25*(8), 861–875. <https://dx.doi.org/10.1071/WF15026>
- Cai, W. H., Yang, J., Liu, Z. H., Hu, Y. M., & Weisberg, P. J. (2013). Post-fire tree recruitment of a boreal larch forest in Northeast China. *Forest Ecology and Management*, *307*, 20–29. <https://dx.doi.org/10.1016/j.foreco.2013.06.056>
- Cai, W. H., Yang, Y. Z., Yang, J., & He, H. S. (2018). Topographic variation in the climatic change response of a larch forest in northeastern China. *Landscape Ecology*, *33*, 2013–2029. <https://doi.org/10.1007/s10980-018-0711-3>
- Camac, J. S., Williams, R. J., Wahren, C. H., Hoffmann, A. A., & Vesik, P. A. (2017). Climatic warming strengthens a positive feedback between alpine shrubs and fire. *Global Change Biology*, *23*(8), 3249–3258. <https://doi.org/10.1111/gcb.13614>
- Chang, Y., He, H. S., Hu, Y. M., Bu, R. C., & Li, X. Z. (2008). Historic and current fire regimes in the Great Xing'an Mountains, northeastern China: Implications for long-term forest management. *Forest Ecology and Management*, *254*(3), 445–453. <https://doi.org/10.1016/j.foreco.2007.04.050>
- Chapin, F. S. III, Matson, P. A., & Vitousek, P. (2011). *Principles of terrestrial ecosystem ecology*. New York: Springer. <https://doi.org/10.1007/978-1-4419-9504-9>
- Chapin, F. S. III, Woodwell, G. M., Randerson, J. T., Rastetter, E. B., Lovett, G. M., Baldocchi, D. D., et al. (2006). Reconciling carbon-cycle concepts, terminology, and methods. *Ecosystems*, *9*(7), 1041–1050. <https://doi.org/10.1007/s10021-005-0105-7>
- Chen, G. S., Yang, Z. J., Gao, R., Xie, J. S., Guo, J. F., Huang, Z. Q., & Yang, Y. S. (2013). Carbon storage in a chronosequence of Chinese fir plantations in southern China. *Forest Ecology and Management*, *300*, 68–76. <https://doi.org/10.1016/j.foreco.2012.07.046>
- Clemmensen, K. E., Bahr, A., Ovaskainen, O., Dahlberg, A., Ekblad, A., Wallander, H., et al. (2013). Roots and associated fungi drive long-term carbon sequestration in boreal forest. *Science*, *339*(6127), 1615–1618. <https://doi.org/10.1126/science.1231923>
- Clemmensen, K. E., Finlay, R. D., Dahlberg, A., Stenlid, J., Wardle, D. A., & Lindahl, B. D. (2015). Carbon sequestration is related to mycorrhizal fungal community shifts during long-term succession in boreal forests. *New Phytologist*, *205*(4), 1525–1536. <https://doi.org/10.1111/nph.13208>
- Covington, W. W. (1981). Changes in forest floor organic matter and nutrient content following clear cutting in northern hardwoods. *Ecology*, *62*(1), 41–48. <https://doi.org/10.2307/1936666>
- Dale, V. H., Joyce, L. A., McNulty, S., Neilson, R. P., Ayres, M. P., Flannigan, M. D., et al. (2001). Climate change and forest disturbances. *Bioscience*, *51*(9), 723–734. [https://doi.org/10.1641/0006-3568\(2001\)051\[0723:CCAFD\]2.0.CO;2](https://doi.org/10.1641/0006-3568(2001)051[0723:CCAFD]2.0.CO;2)
- de Groot, W. J., Cantin, A. S., Flannigan, M. D., Soja, A. J., Gowman, L. M., & Newbery, A. (2013). A comparison of Canadian and Russian boreal forest fire regimes. *Forest Ecology and Management*, *294*, 23–34. <https://doi.org/10.1016/j.foreco.2012.07.033>
- de Groot, W. J., Flannigan, M. D., & Cantin, A. S. (2013). Climate change impacts on future boreal fire regimes. *Forest Ecology and Management*, *294*, 35–44. <https://doi.org/10.1016/j.foreco.2012.09.027>
- de Groot, W. J., Pritchard, J. M., & Lynham, T. J. (2009). Forest floor fuel consumption and carbon emissions in Canadian boreal forest fires. *Canadian Journal of Forest Research*, *39*(2), 367–382. <https://doi.org/10.1139/x08-192>
- Donato, D. C., Fontaine, J. B., Campbell, J. L., Robinson, W. D., Kauffman, J. B., & Law, B. E. (2009). Conifer regeneration in stand-replacement portions of a large mixed-severity wildfire in the Klamath-Siskiyou Mountains. *Canadian Journal of Forest Research*, *39*(4), 823–838. <https://doi.org/10.1139/x09-016>
- Fang, L., Yang, J., Zu, J. X., Li, G. C., & Zhang, J. S. (2015). Quantifying influences and relative importance of fire weather, topography, and vegetation on fire size and fire severity in a Chinese boreal forest landscape. *Forest Ecology and Management*, *356*, 2–12. <https://doi.org/10.1016/j.foreco.2015.01.011>
- Flannigan, M. D. (2015). Carbon cycle: Fire evolution split by continent. *Nature Geoscience*, *8*, 167–168. <https://doi.org/10.1038/ngeo2360>
- Flannigan, M. D., Logan, K. A., Amiro, B. D., Skinner, W. R., & Stocks, B. J. (2005). Future area burned in Canada. *Climatic Change*, *72*, 1–16. <https://doi.org/10.1007/s1084-005-5935-y>
- Flannigan, M. D., Stocks, B. J., Turetsky, M. R., & Wotton, M. B. (2009). Impacts of climate change on fire activity and fire management in the circumboreal forest. *Global Change Biology*, *15*(3), 549–560. <https://doi.org/10.1111/j.1365-2486.2008.01660.x>
- Flannigan, M. D., Wotton, B. M., Marshall, G. A., de Groot, W. J., Johnston, J., Jurko, N., & Cantin, A. S. (2016). Fuel moisture sensitivity to temperature and precipitation: Climate change implications. *Climate Change*, *134*(1–2), 59–71. <https://doi.org/10.1007/s10584-015-1521-0>

- Freschet, G. T., Weedon, J. T., Aerts, R., van Hal, J. R., & Cornelissen, J. H. C. (2012). Interspecific differences in wood decay rates: Insights from a new short-term method to study long-term wood decomposition. *Journal of Ecology*, *100*(1), 161–170. <https://doi.org/10.1111/j.1365-2745.2011.01896.x>
- Gao, B., Taylor, A. R., Searle, E. B., Kumar, P., Ma, Z., Hume, A. M., & Chen, H. Y. H. (2018). Carbon storage declines in old boreal forests irrespective of succession pathway. *Ecosystems*, *21*(6), 1168–1182. <https://doi.org/10.1007/s10021-017-0210-4>
- Girardin, M. P., Ali, A. A., Carcaillet, C., Mudelsee, M., Drobyshev, I., Hély, C., & Bergeron, Y. (2009). Heterogeneous response of circumboreal wildfire risk to climate change since the early 1900s. *Global Change Biology*, *15*(11), 2751–2769. <https://doi.org/10.1111/j.1365-2486.2009.01869.x>
- Goetz, S. J., Mack, M. C., Gurney, K. R., Randerson, J. T., & Houghton, R. A. (2007). Ecosystem responses to recent climate change and fire disturbance at northern high latitudes: Observations and model results contrasting northern Eurasia and North America. *Environmental Research Letters*, *2*(4), 045031. <https://doi.org/10.1088/1748-9326/2/4/045031>
- Gough, C. M., Vogel, C. S., Kazanski, C., Nagel, L., Flower, C. E., & Curtis, P. S. (2007). Coarse woody debris and the carbon balance of a north temperate forest. *Forest Ecology and Management*, *244*, 60–67. <https://doi.org/10.1016/j.foreco.2007.03.039>
- Gower, S. T., Krankina, O., Olson, R. J., Apps, M., Linder, S., & Wang, C. (2001). Net primary production and carbon allocation patterns of boreal forest ecosystems. *Ecological Applications*, *11*(5), 1395–1411. [https://doi.org/10.1890/1051-0761\(2001\)011\[1395:NPPACA\]2.0.CO;2](https://doi.org/10.1890/1051-0761(2001)011[1395:NPPACA]2.0.CO;2)
- Harden, J., Trumbore, S., Stocks, B., Hirsch, A., Gower, S., O'Neill, K., & Kasischke, E. (2000). The role of fire in the boreal carbon budget. *Global Change Biology*, *6*(S1), 174–184. <https://doi.org/10.1046/j.1365-2486.2000.06019.x>
- Harris, R., Remenyi, T. A., Williamson, G. J., Bindoff, N. L., & Bowman, D. M. (2016). Climate–vegetation–fire interactions and feedbacks: Trivial detail or major barrier to projecting the future of the Earth system? *Wiley Interdisciplinary Reviews: Climate Change*, *7*(6), 910–931. <https://doi.org/10.1002/wcc.428>
- Hart, S. A., & Chen, H. Y. H. (2008). Fire, logging, and overstory affect understory abundance, diversity, and composition in boreal forest. *Ecological Monographs*, *78*(1), 123–140. <https://doi.org/10.1890/06-2140.1>
- Harvey, B. J., Donato, D. C., & Turner, M. G. (2016a). Burn me twice, shame on who? Interactions between successive forest fires across a temperate mountain region. *Ecology*, *97*(9), 2272–2282. <https://doi.org/10.1002/ecy.1439>
- Harvey, B. J., Donato, D. C., & Turner, M. G. (2016b). High and dry: Post-fire tree seedling establishment in subalpine forests decreases with post-fire drought and large stand-replacing burn patches. *Global Ecology and Biogeography*, *25*(6), 655–669. <https://doi.org/10.1111/geb.12443>
- Harwell, M. A., Cropper, W. P., & Ragsdale, H. L. (1977). Nutrient recycling and stability: A reevaluation. *Ecology*, *58*(3), 660–666. <https://doi.org/10.2307/1939016>
- Hayes, D. J., McGuire, A. D., Kicklighter, D. W., Gurney, K. R., Burnside, T., & Melillo, J. M. (2011). Is the northern high-latitude land-based CO₂ sink weakening? *Global Biogeochemical Cycles*, *25*, GB3018. <https://doi.org/10.1029/2010GB003813>
- Hogg, E. H., & Michaelian, M. (2015). Factors affecting fall down rates of dead aspen (*Populus tremuloides*) biomass following severe drought in west-central Canada. *Global Change Biology*, *21*(5), 1968–1979. <https://doi.org/10.1111/gcb.12805>
- Holland, G. J., Clarke, M. F., & Bennett, A. F. (2017). Prescribed burning consumes key forest structural components: Implications for landscape heterogeneity. *Ecological Applications*, *27*(3), 845–858. <https://doi.org/10.1002/eap.1488>
- Houghton, R. A. (2005). Aboveground forest biomass and the global carbon balance. *Global Change Biology*, *11*(6), 945–958. <https://doi.org/10.1111/j.1365-2486.2005.0055.x>
- Hurteau, M. D., & Brooks, M. L. (2011). Short- and long-term effects of fire on carbon in US dry temperature forest systems. *Bioscience*, *61*(2), 139–146. <https://doi.org/10.1525/bio.2011.62.2.9>
- Janisch, J. E., & Harmon, M. E. (2002). Successional changes in live and dead wood carbon stores: Implications for net ecosystem productivity. *Tree Physiology*, *22*(2–3), 77–89. <https://doi.org/10.1093/treephys/22.2-3.77>
- Jasinski, J. P. P., & Payette, S. (2005). The creation of alternative stable states in the southern boreal forest, Québec, Canada. *Ecological Monographs*, *75*(4), 561–583. <https://doi.org/10.1890/04-1621>
- Jiao, Y. (2006). Carbon release of dominant shrubs, herbaceous and forest floor in Great Xing'an Mountains, (master's thesis). Northeast Forestry University, China.
- Johnstone, J. F., Allen, C. D., Franklin, J. F., Frelich, L. E., Harvey, B. J., Higuera, P. E., et al. (2016). Changing disturbance regimes, ecological memory, and forest resilience. *Frontiers in Ecology and the Environment*, *14*(7), 369–378. <https://doi.org/10.1002/fee.1311>
- Johnstone, J. F., & Chapin, F. S. III (2006). Effects of soil burn severity on post-fire tree recruitment in boreal forest. *Ecosystems*, *9*(1), 14–31. <https://doi.org/10.1007/s10021-004-0042-x>
- Johnstone, J. F., Chapin, F. S. III, Foote, J., Kemmett, S., Price, K., & Viereck, L. (2004). Decadal observations of tree regeneration following fire in boreal forests. *Canadian Journal of Forest Research*, *34*(2), 267–273. <https://doi.org/10.1139/x03-183>
- Johnstone, J. F., Hollingsworth, T. N., Chapin, F. S. III, & Mack, M. C. (2010). Changes in fire regime break the legacy lock on successional trajectories in Alaskan boreal forest. *Global Change Biology*, *16*(4), 1281–1295. <https://doi.org/10.1111/j.1365-2486.2009.02051.x>
- Johnstone, J. F., & Kasischke, E. S. (2005). Stand-level effects of soil burn severity on postfire regeneration in a recently burned black spruce forest. *Canadian Journal of Forest Research*, *35*(9), 2151–2163. <https://doi.org/10.1139/x05-087>
- Kajimoto, T. (1989). Aboveground biomass and litterfall of *Pinus pumila* scrubs growing on the Kiso mountain range in central Japan. *Ecological Research*, *4*(1), 55–69. <https://doi.org/10.1007/BF02346943>
- Kajimoto, T. (1992). Dynamics and dry matter production of belowground woody organs of *Pinus pumila* trees growing on the Kiso mountain range in central Japan. *Ecological Research*, *7*(3), 333–339. <https://doi.org/10.1007/BF02347100>
- Kang, L. (2012). A study on the decomposition of fallen trees of *Larix gmelinii* and *Betula platyphylla* forests in Daxinganling Mountains, (master's thesis). Inner Mongolia Agricultural University, China.
- Kashian, D. M., Romme, W. H., Tinker, D. B., Turner, M. G., & Ryan, M. G. (2006). Carbon storage on landscapes with stand-replacing fires. *Bioscience*, *56*(7), 598–606. [https://doi.org/10.1641/0006-3568\(2006\)56\[598:CSLWSJ\]2.0.CO;2](https://doi.org/10.1641/0006-3568(2006)56[598:CSLWSJ]2.0.CO;2)
- Kashian, D. M., Romme, W. H., Tinker, D. B., Turner, M. G., & Ryan, M. G. (2013). Postfire changes in forest carbon storage over a 300-year chronosequence of *Pinus contorta*-dominated forests. *Ecological Monographs*, *83*(1), 49–66. <https://doi.org/10.1890/11-1454.1>
- Kashian, D. M., Tinker, D. B., Turner, M. G., & Scarpace, F. L. (2004). Spatial heterogeneity of lodgepole pine sapling densities following the 1988 fires in Yellowstone National Park, Wyoming, USA. *Canadian Journal of Forest Research*, *34*(11), 2263–2276. <https://doi.org/10.1139/x04-107>
- Kashian, D. M., Turner, M. G., Romme, W. H., & Lorimer, C. G. (2005). Variability and convergence in stand structural development on a fire-dominated subalpine landscape. *Ecology*, *86*(3), 643–654. <https://doi.org/10.1890/03-0828>
- Kaye, J. P., Romanya, J., & Vallejo, V. R. (2010). Plant and soil carbon accumulation following fire in Mediterranean woodlands in Spain. *Oecologia*, *164*(2), 533–543. <https://doi.org/10.1007/s00442-010-1659-4>

- Kelly, R., Chipman, M. L., Higuera, P. E., Stefanova, I., Brubaker, L. B., & Hu, F. S. (2013). Recent burning of boreal forests exceeds fire regime limits of the past 10,000 years. *Proceedings of the National Academy of Sciences of the United States of America*, *110*(32), 13,055–13,060. <https://doi.org/10.1073/pnas.1305069110>
- Kobak, K. I., Turchinovich, I. Y., Kondrasheva, N. Y., Schulze, E. D., Schulze, W., Koch, H., & Vygodskaya, N. N. (1996). Vulnerability and adaptation of the larch forest in eastern Siberia to climate change. *Water, Air, and Soil Pollution*, *92*(1–2), 119–127. <https://doi.org/10.1007/BF00175558>
- Kong, J. J., Yang, J., Chu, H. Y., & Xiang, X. J. (2015). Effects of wildfire and topography on soil nitrogen availability in a boreal larch forest of northeastern China. *International Journal of Wildland Fire*, *24*(3), 433–442. <https://doi.org/10.1071/WF13218>
- Law, B. E., Sun, O. J., Campbell, J., Van Tuyl, S., & Thornton, P. E. (2003). Changes in carbon storage and fluxes in a chronosequence of ponderosa pine. *Global Change Biology*, *9*(4), 510–524. <https://doi.org/10.1046/j.1365-2486.2003.00624.x>
- Li, Z. (2013). Biomass and carbon storage of the *Larix gmelinii* forest's research, (master's thesis). Inner Mongolia Agricultural University, China.
- Liu, S. G., Bond-Lamberty, B., Hicke, J. A., Vargas, R., Zhao, S. Q., Chen, J., et al. (2011). Simulating the impacts of disturbances on forest carbon cycling in North America: Processes, data, models, and challenges. *Journal of Geophysical Research*, *116*, G00K08. <https://doi.org/10.1029/2010JG001585>
- Liu, Z. H., Yang, J., Chang, Y., Weisberg, P. J., & He, H. S. (2012). Spatial patterns and drivers of fire occurrence and its future trend under climate change in a boreal forest of Northeast China. *Global Change Biology*, *18*(6), 2041–2056. <https://doi.org/10.1111/j.1365-2486.2012.02649.x>
- Luo, Y., Keenan, T. F., & Smith, M. (2015). Predictability of the terrestrial carbon cycle. *Global Change Biology*, *21*(5), 1737–1751. <https://doi.org/10.1111/gcb.12766>
- Luysaert, S., Inglima, I., Jung, M., Richardson, A. D., Reichstein, M., Papale, D., et al. (2007). CO₂ balance of boreal, temperate, and tropical forests derived from a global database. *Global Change Biology*, *13*(12), 2509–2537. <https://doi.org/10.1111/j.1365-2486.2007.01439.x>
- Luysaert, S., Schulze, E. D., Börner, A., Knohl, A., Hessenmöller, D., Law, B. E., et al. (2008). Old-growth forests as global carbon sinks. *Nature*, *455*, 213–215. <https://doi.org/10.1038/nature07276>
- Mack, M. C., Bret-Harte, M. S., Hollingsworth, T. N., Jandt, R. R., Schuur, E. A., Shaver, G. R., & Verbyla, D. L. (2011). Carbon loss from an unprecedented Arctic tundra wildfire. *Nature*, *475*, 489–492. <https://doi.org/10.1038/nature10283>
- Mack, M. C., Treseder, K. K., Manies, K. L., Harden, J. W., Schuur, E. A. G., Vogel, J. G., et al. (2008). Recovery of aboveground plant biomass and productivity after fire in mesic and dry black spruce forests of interior Alaska. *Ecosystems*, *11*(2), 209–225. <https://doi.org/10.1007/s10021-007-9117-9>
- Manies, K. L., Harden, J. W., Bond-Lamberty, B., & O'Neill, K. P. (2005). Woody debris along an upland chronosequence in boreal Manitoba and its impact on long-term carbon storage. *Canadian Journal of Forest Research*, *35*(2), 472–482. <https://doi.org/10.1139/x04-179>
- Matamala, R., Jastrow, J. D., Miller, R. M., & Garten, C. (2008). Temporal changes in C and N stocks of restored prairie: Implications for C sequestration strategies. *Ecological Applications*, *18*(6), 1470–1488. <https://doi.org/10.1890/07-1609.1>
- Mkhabela, M., Amiro, B. D., Barr, A. G., Black, T. A., Hawthorne, I., Kidston, J., et al. (2009). Comparison of carbon dynamics and water use efficiency following fire and harvesting in Canadian boreal forests. *Agricultural and Forest Meteorology*, *149*(5), 783–794. <https://doi.org/10.1016/j.agrformet.2008.10.025>
- Murphy, B. P., Cochrane, M. A., & Russell-Smith, J. (2015). Prescribed burning protects endangered tropical heathlands of the Arnhem Plateau, northern Australia. *Journal of Applied Ecology*, *52*(4), 980–991. <https://doi.org/10.1111/1365-2664.12455>
- Nemani, R. R., Keeling, C. D., Hashimoto, H., Jolly, W. M., Piper, S. C., Tucker, C. J., et al. (2003). Climate-driven increases in global terrestrial net primary production from 1982 to 1999. *Science*, *300*(5625), 1560–1563. <https://doi.org/10.1126/science.1082750>
- Oliver, C. D., & Larson, B. C. (1996). *Forest stand dynamics: Updated edition, John*. New York: Wiley and Sons.
- Ortiz, M., & Wolff, M. (2002). Dynamical simulation of mass-balance trophic models for benthic communities of north-central Chile: Assessment of resilience time under alternative management scenarios. *Ecological Modelling*, *148*(3), 277–291. [https://doi.org/10.1016/S0304-3800\(01\)00454-9](https://doi.org/10.1016/S0304-3800(01)00454-9)
- Osawa, A., Zyryanova, O. A., Matsuura, Y., Kajimoto, T., & Wein, R. W. (2010). *Permafrost ecosystems: Siberian larch forests*. New York: Springer. <https://doi.org/10.1007/978-1-4020-9693-8>
- Pan, Y., Birdsey, R. A., Fang, J. Y., Houghton, R., Kauppi, P. E., Kurz, W. A., et al. (2011). A large and persistent carbon sink in the world's forests. *Science*, *333*(6045), 988–993. <https://doi.org/10.1126/science.1201609>
- Pellegrini, A. F. A., Ahlstrom, A., Hobbie, S. E., Reich, P. B., Nieradzik, L. P., Staver, A. C., et al. (2017). Fire frequency drives decadal changes in soil carbon and nitrogen and ecosystem productivity. *Nature*, *553*, 194–198. <https://doi.org/10.1038/nature24668>
- R Development Core Team (2017). *R: A language and environment for statistical computing. Version 3.4.0*. Vienna, Austria: R Foundation for Statistical Computing.
- Randerson, J. T., Liu, H., Flanner, M. G., Chambers, S. D., Jin, Y., Hess, P. G., et al. (2006). The impact of boreal forest fire on climate warming. *Science*, *314*(5802), 1130–1132. <https://doi.org/10.1126/science.1132075>
- Riaño, D., Moreno Ruiz, J. A., Barón Martínez, J., & Ustin, S. L. (2007). Burned area forecasting using past burned area records and Southern Oscillation Index for tropical Africa (1981–1999). *Remote Sensing of Environment*, *107*(4), 571–581. <https://doi.org/10.1016/j.rse.2006.10.008>
- Rogers, B. M., Soja, A. J., Goulden, M. L., & Randerson, J. T. (2015). Influence of tree species on continental differences in boreal fires and climate feedbacks. *Nature Geoscience*, *8*, 228–234. <https://doi.org/10.1038/ngeo2352>
- Rothstein, D. E., Yermakov, Z., & Buell, A. L. (2004). Loss and recovery of ecosystem carbon pools following stand-replacing wildfire in Michigan jack pine forests. *Canadian Journal of Forest Research*, *34*(9), 1908–1918. <https://doi.org/10.1139/x04-063>
- Russell, M. B., Woodall, C. W., Fraver, S., D'Amato, A. W., Domke, G. M., & Skog, K. E. (2014). Residence times and decay rates of downed woody debris biomass/carbon in eastern US forests. *Ecosystems*, *17*(5), 765–777. <https://doi.org/10.1007/s10021-014-9757-5>
- Santin, C., Doerr, S. H., Preston, C. M., & Gonzalez-Rodriguez, G. (2015). Pyrogenic organic matter production from wildfires: A missing sink in the global carbon cycle. *Global Change Biology*, *21*(4), 1621–1633. <https://doi.org/10.1111/gcb.12800>
- Seedre, M., Taylor, A. R., Brassard, B. W., Chen, H. Y. H., & Jögiste, K. (2014). Recovery of ecosystem carbon stocks in young boreal forests: A comparison of harvesting and wildfire disturbance. *Ecosystems*, *17*(5), 851–863. <https://doi.org/10.1007/s10021-014-9763-7>
- Seidl, R., Spies, T. A., Peterson, D. L., Stephens, S. L., & Hicke, J. A. (2016). Searching for resilience: Addressing the impacts of changing disturbance regimes on forest ecosystem services. *Journal of Applied Ecology*, *53*(1), 120–129. <https://doi.org/10.1111/1365-2664.12511>
- Shenoy, A., Johnstone, J. F., Kasischke, E. S., & Kielland, K. (2010). Persistent effects of fire severity on early successional forests in interior Alaska. *Forest Ecology and Management*, *261*(3), 381–390. <https://doi.org/10.1016/j.foreco.2010.10.021>
- Stephens, S. L., Burrows, N., Buyantuyev, A., Gray, R. W., Keane, R. W., Kubian, R., et al. (2014). Temperate and boreal forest mega-fires: Characteristics and challenges. *Frontiers in Ecology and the Environment*, *12*(2), 115–122. <https://doi.org/10.1890/120332>

- Stevens, J. T., & Latimer, A. M. (2015). Snowpack, fire, and forest disturbance: Interactions affect montane invasions by non-native shrubs. *Global Change Biology*, 21(6), 2379–2393. <https://doi.org/10.1111/gcb.12824>
- Stinson, G., Kurz, W. A., Smyth, C. E., Neilson, E. T., Dymond, C. C., Metsaranta, J. M., et al. (2011). An inventory-based analysis of Canada's managed forest carbon dynamics, 1990 to 2008. *Global Change Biology*, 17(6), 2227–2244. <https://doi.org/10.1111/j.1365-2486.2010.02369.x>
- Taylor, A. R., Wang, J. R., & Chen, H. Y. H. (2007). Carbon storage in a chronosequence of red spruce (*Picea rubens*) forests in central Nova Scotia, Canada. *Canadian Journal of Forest Research*, 37(11), 2260–2269. <https://doi.org/10.1139/x07-080>
- Taylor, C., McCarthy, M. A., & Lindenmayer, D. B. (2014). Nonlinear effects of stand age on fire severity. *Conservation Letters*, 7(4), 355–370. <https://doi.org/10.1111/conl.12122>
- Tepley, A. J., Veblen, T. T., Perry, G. L. W., Stewart, G. H., & Naficy, C. E. (2016). Positive feedbacks to fire-driven deforestation following human colonization of the South Island of New Zealand. *Ecosystems*, 19(8), 1325–1344. <https://doi.org/10.1007/s10021-016-0008-9>
- Turner, M. G., Tinker, D. B., Romme, W. H., Kashian, D. M., & Litton, C. M. (2004). Landscape patterns of sapling density, leaf area, and aboveground net primary production in postfire lodgepole pine forests, Yellowstone National Park (USA). *Ecosystems*, 7, 751–775. <https://doi.org/10.1007/s10021-004-0011-4>
- Turner, M. G., Whitby, T. G., Tinker, D. B., & Romme, W. H. (2016). Twenty-four years after the Yellowstone Fires: Are postfire lodgepole pine stands converging in structure and function? *Ecology*, 97(5), 1260–1273. <https://doi.org/10.1890/15-1585.1>
- Usoltsev, V. A., Koltunova, A. L., Kajimoto, T., Osawa, A., & Koike, T. (2002). Geographical gradients of annual biomass production from larch forests in northern Eurasia. *European Journal of Forest Research*, 5, 55–62. <http://hdl.handle.net/2115/22150>
- Vijayakumar, D. B. I. P., Raulier, F., Bernier, P., Pare, D., Gauthier, S., Bergeron, Y., & Pothier, D. (2016). Cover density recovery after fire disturbance controls landscape aboveground biomass carbon in the boreal forest of eastern Canada. *Forest Ecology and Management*, 360, 170–180. <https://doi.org/10.1016/j.foreco.2015.10.035>
- Walker, L. R., Wardle, D. A., Bardgett, R. D., & Clarkson, B. D. (2010). The use of chronosequences in studies of ecological succession and soil development. *Journal of Ecology*, 98(4), 725–736. <https://doi.org/10.1111/j.1365-2745.2010.01664.x>
- Wang, C. K. (2006). Biomass allometric equations for 10 co-occurring tree species in Chinese temperate forests. *Forest Ecology and Management*, 222(1–3), 9–16. <https://doi.org/10.1016/j.foreco.2005.10.074>
- Wang, C. K., Bond-Lamberty, B., & Gower, S. T. (2003). Carbon distribution of a well- and poorly-drained black spruce fire chronosequence. *Global Change Biology*, 9(7), 1066–1079. <https://doi.org/10.1046/j.1365-2486.2003.00645.x>
- Wang, C. K., Gower, S. T., Wang, Y. H., Zhao, H. X., Yan, P., & Bond-Lamberty, B. (2001). The influence of fire on carbon distribution and net primary production of boreal *Larix gmelinii* forests in north-eastern China. *Global Change Biology*, 7(6), 719–730. <https://doi.org/10.1046/j.1354-1013.2001.00441.x>
- Wang, X. L., Thompson, D. K., Marshall, G. A., Tymstra, C., Carr, R., & Flannigan, M. D. (2015). Increasing frequency of extreme fire weather in Canada with climate change. *Climatic Change*, 130(4), 573–586. <https://doi.org/10.1007/s10584-015-1375-5>
- White, L. L., Zak, D. R., & Barnes, B. V. (2004). Biomass accumulation and soil nitrogen availability in an 87-year-old *Populus grandidentata* chronosequence. *Forest Ecology and Management*, 191(1–3), 121–127. <https://doi.org/10.1016/j.foreco.2003.11.010>
- Williams, C. A., Collatz, G. J., Masek, J., & Goward, S. N. (2012). Carbon consequences of forest disturbance and recovery across the conterminous United States. *Global Biogeochemical Cycles*, 26, GB1005. <https://doi.org/10.1029/2010GB003947>
- Wirth, C., Schulze, E. D., Luhker, B., Grigoriev, S., Siry, M., Harges, G., et al. (2002). Fire and site type effects on the long-term carbon and nitrogen balance in pristine Siberian Scots pine forests. *Plant and Soil*, 242(1), 41–63. <https://doi.org/10.1023/A:1020813505203>
- Xu, H. C. (1998). *Forest in Great Xing'An Mountains of China*. Beijing: China, Science Press.
- Xu, H. C., Li, Z. D., & Qiu, Y. (1997). Fire disturbance history in virgin forest in northern region of Daxinganling Mountains. *Acta Ecologica Sinica*, 17(4), 337–343.
- Yang, Y., Luo, Y., & Finzi, A. C. (2011). Carbon and nitrogen dynamics during forest stand development: A global synthesis. *New Phytologist*, 190(4), 977–989. <https://doi.org/10.1111/j.1469-8137.2011.03645.x>
- Zak, D. R., Grigal, D. F., Gleeson, S., & Tilman, D. (1990). Carbon and nitrogen cycling during old-field succession: Constraints on plant and microbial biomass. *Biogeochemistry*, 11(2), 111–129. <https://doi.org/10.1007/BF00002062>
- Zhang, Q. Z., Wang, C. K., Wang, X. C., & Quan, X. K. (2009). Carbon concentration variability of 10 Chinese temperate tree species. *Forest Ecology and Management*, 258(5), 722–727. <https://doi.org/10.1016/j.foreco.2009.05.009>
- Zhou, Y. L., Ai, C. L., Dong, S. L., Nie, S. Q., & Yang, G. T. (1991). *Vegetation of Da Hinggan Ling in China*. Beijing: China, Science Press.